

In Situ Spectroscopic and Microscopic Study on Dispersion of Ag Nanoparticles in Polymer Thin Films

Kensuke Akamatsu,[†] Nobuo Tsuboi,[‡] Yoshinori Hatakenaka,[‡] and Shigehito Deki^{*,‡}

Division of Molecular Science, Graduate School of Science and Technology, Kobe University, Rokkodai, Nada, Kobe 657-8501, Japan, Department of Chemical Science & Engineering, Faculty of Engineering, Kobe University, Rokkodai, Nada, Kobe 657-8501, Japan

Received: April 26, 2000; In Final Form: August 21, 2000

The dispersion process of Ag nanoparticles into vapor-deposited nylon 11 thin films caused by heat treatment has been investigated. In situ optical transmission and Fourier transform infrared (FT-IR) reflection absorption spectroscopy were used independently for characterizing the changes in the surface plasmon resonance response of Ag nanoparticles and in the thermal behavior of the nylon 11 matrix during heat treatment, respectively. The peak wavelength of the plasmon band was observed to shift to shorter wavelength in the temperature range 40–80 °C. The infrared temperature study revealed that the as-deposited nylon 11 matrix is thermodynamically metastable and semicrystalline, including hydrogen-bonded small crystallites. These relaxed upon heat treatment above 40 °C, at which the Ag nanoparticles penetrated from the surface into the bulk phase of the matrix. These results demonstrate that there is a strong correlation between the optical spectral features, dispersion state of the particles, and structural change of the polymer matrix. Dispersion mechanism is discussed in terms of the surface free energy of Ag nanoparticles, which is reduced upon embedding in the polymer matrix.

Introduction

The study of optical properties of the composite films consisting of metallic particles dispersed in solid dielectric materials has received considerable interest in recent years, because such materials possess exciting possibilities for potential device applications based on quantum size effects. It is well-known that the nanometer-sized metallic particles exhibit the optical absorption in the ultraviolet–visible region due to the excitation of the surface plasmon resonance modes.^{1,2} The plasmon absorption characteristics of the composite films are also known to be very sensitive to the microstructure of the film, e.g., particle size, shape, and three-dimensional distribution of the particles in the film.^{3–8} Generally, the plasmon modes have been characterized by means of conventional optical transmission^{1–8} as well as attenuated total reflection spectroscopy.^{9–11} On the other hand, lateral and cross-sectional transmission electron microscopy (TEM) are the primary techniques used for characterizing the structure and distribution of the metallic particles. Therefore, analysis for the spectral features of the plasmon absorption and characterization of the microstructure by using microscopic techniques are of great importance to fully understand the relationship between structure and optical properties of the composite films.

We have previously developed a novel technique to prepare composite thin film consisting of the nanosized metallic particles embedded homogeneously in polymer matrix.^{12–14} This technique relies on consecutive vacuum vapor deposition of a polymer and a metal followed by heat treatment. The heat treatment above the glass transition temperature (T_g) of the

polymer matrix induces the structural rearrangement of polymer matrix, initially fixed with thermodynamically metastable structure. It was shown that in this process the upper metal layer (or islands) can be dispersed into the polymer phase as nanosized particles with relatively narrow size distribution. Due to the chemical stability and strong interaction with metals, the polyamide group polymers have been chosen for the preparation of the composite film. We have shown that the size of the dispersed particles and concentration of the metal phase could be systematically controlled by changing the initial amount of metal deposition and thickness of the polymer matrix. However, knowledge of the details of the dispersion mechanism of metal particles from surface into bulk phase of the polymer matrix is still incomplete. In the previous work, we have studied changes in the optical absorption of Au/nylon 11 system in relation to the dispersion state of the Au nanoparticles as a function of temperature.¹⁵ It was shown that, as the Au nanoparticles disperse from surface into bulk phase of the nylon 11 matrix by the heat treatment, the plasmon absorption peak position and intensity of the Au nanoparticles shift to shorter wavelengths and decrease, respectively. This behavior is explained by the dipole interaction between neighboring nanoparticles. Recently, we have investigated the effect of heat treatment on the dispersion state of Au nanoparticles by using cross-sectional TEM observation.¹⁶ The Au nanoparticles were found to penetrate into amorphous phase of the nylon 11 matrix by the heat treatment while initially amorphous nylon 11 matrix transformed partially into α -crystalline phase. It was shown that the structural rearrangement of the polymer matrix plays an important role for the penetration of the nanoparticles during heat treatment. The structural change of the polymer matrix caused by heat treatment was analyzed so far at room temperature because of experimental difficulty for investigating the structure of thin organic polymer films consisted of small atomic weight constituent by conventional X-ray and electron diffrac-

* Corresponding author. Tel(Fax): +(81)78-803-6160. E-mail: deki@kobe-u.ac.jp.

[†] Division of Molecular Science, Graduate School of Science and Technology, Kobe University.

[‡] Department of Chemical Science & Engineering, Faculty of Engineering, Kobe University.

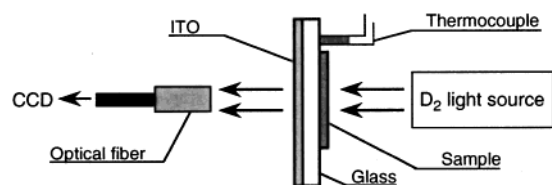


Figure 1. Experimental arrangement of the in situ optical transmission measurement for Ag/nylon 11 specimen during heat treatment.

tion techniques. However, to elucidate the dispersion mechanism, it is necessary to investigate the temperature dependence of the structural change of the polymer matrix by in situ measurement and compare the results with dispersion state of the nanoparticles.

In this paper, we investigate the changes in the optical absorption of the Ag/nylon 11 system during heat treatment by using a charge-coupled device (CCD) analyzer. The Ag nanoparticles are known to exhibit relatively strong plasmon absorption in the visible region as compared with Au nanoparticles because the interband transition of Ag is in the near-ultraviolet region while that of Au is superpositioned at the plasmon frequency of Au particles.¹⁷ Therefore, the plasmon peak position, intensity, and width for Ag nanoparticles can be determined more precisely than the Au nanoparticles. The distribution of the Ag nanoparticles in the nylon 11 matrix was characterized by cross-sectional TEM observation. We have also studied the effect of heat treatment on the structure of the nylon 11 matrix by means of Fourier-transform infrared (FT-IR) reflection absorption spectroscopy. The conformationally sensitive amide I mode related to the hydrogen-bonded carbonyl groups is studied as a function of temperature. It is shown that there are strong correlations between the changes in the optical and IR absorption spectra during heat treatment. Combining the results obtained by TEM observation, we also discuss the dispersion mechanism of the Ag nanoparticles in the film during heat treatment.

Experimental Section

Deposition of Films. Ag/nylon 11 films were prepared by conventional vacuum evaporation technique, similar to those used in our previous studies on Au nanoparticles dispersed in nylon 11 matrixes.¹⁴ A glass vacuum evaporation chamber was initially evacuated to below 1.0×10^{-5} Torr, and nylon 11 pellets (Aldrich) were evaporated using a resistance-heated molybdenum boat at a pressure of 4.0×10^{-4} Torr. The thickness of the nylon 11 matrix was ca. 100 nm as monitored by a quartz-crystal microbalance. Ag metal (99.99%) was then vapor deposited on the nylon 11 film at room temperature using an alumina basket at 2.0×10^{-5} Torr with a deposition rate of 0.5 \AA/s . The amount of deposited Ag was set to $11.8 \times 10^{15} \text{ atom/cm}^2$. In this range, deposited Ag layer consists of islands of roughly spherical shape, since this amount is insufficient to achieve continuous film.

In Situ Optical Transmission Measurement. For in situ optical transmission measurements, an indium tin oxide (ITO)-coated glass substrate which acts as a semiconductor heater was used for film deposition and cleaned with detergent, acetone, and distilled water prior to use. The experimental setup for transmission measurements is schematically shown in Figure 1. The samples prepared on the ITO glass substrate were mounted on a Teflon stage, and Cu electrode was connected onto ITO with the aid of silver paste. The samples were heated at a constant rate of $0.9 \text{ }^\circ\text{C/min}$. As a light source, a D₂ lamp was used, and the illuminated spot was ca. 5 mm in diameter.

The intensity of transmitted light was measured by a multi-channel CCD spectrophotometer (Hamamatsu Photonics PMA-11-C5966) as a function of temperature. The spectra were recorded at appropriate temperature intervals. Exposure time of the photodetector is 20 ms and number of integration is 100 times. The time required for each measurement is thus 2 s, and temperature rise during this can be negligible ($<0.05 \text{ }^\circ\text{C}$) under the present heating conditions. To obtain the optical absorption spectrum, raw transmitted light intensities were divided by a reference signal, which is the intensity of light transmitted through the ITO glass substrate.

TEM Observation and Electron Diffraction Analysis. The changes in the microstructure of Ag nanoparticles/nylon 11 films caused by heat treatment and selected area electron diffraction (SAED) patterns were observed using JEOL JEM-2010 transmission electron microscope operated at 200 kV. For the characterization of the film microstructure parallel to the substrate, the films were directly deposited on thin carbon films supported on copper mesh grids. For the SAED analysis a selected area aperture with a $1 \mu\text{m}$ diameter was used. The SAED patterns were recorded as an intensity distribution curve. The obtained curves were fitted using a nonlinear least-squares method, and lattice constant of the Ag nanoparticles was determined using (220) diffraction line. The samples for cross-sectional TEM observation were deposited on a cured epoxy resin, according to a previous paper.¹⁶ Thin cross sections with a thickness of ca. 50 nm were obtained with a Leica Ultracut UCT ultramicrotome using a diamond knife. These thin sections floating onto water bath were mounted on the carbon-coated TEM copper grids.

Before TEM observation, all the samples prepared on TEM grids were again coated with a thin carbon layer to prevent electron charging effects during TEM observation.

In Situ IR Measurement. For in situ FT-IR measurement, the samples were deposited on Al pre-deposited glass substrate (Al thickness: 100 nm). The samples were mounted on a ceramic heater stage and set to the attachment. FT-IR spectra were measured by reflection-absorption configuration using FT-IR instrument (FT/IR 615R, Japan Spectroscopic Co.) equipped with an TGS detector. The incident angle was set at 75° , and the light was set to the p polarization with a wire grid polarizer, which was arranged just before the specimen. The spectra were recorded in a range of $400\text{--}4000 \text{ cm}^{-1}$ at a temperature interval of $5 \text{ }^\circ\text{C}$ and at a constant heating rate of $1.0 \text{ }^\circ\text{C/min}$.

Results and Discussion

Changes in the Optical Absorption. During the heat treatment from room temperature up to $100 \text{ }^\circ\text{C}$ at a constant heating rate, the color of the film changed gradually from ruby red to transparent bright yellow. Figure 2 shows the results of in situ transmission measurements for the Ag/nylon 11 film as a function of increasing temperature. The spectra were measured for the specimen with a deposition of $11.8 \times 10^{15} \text{ atoms cm}^{-2}$ and heating rate of $0.9 \text{ }^\circ\text{C min}^{-1}$. In Figure 2, the term $-\log(I/I_0)$ is plotted as a function of the wavelength and the temperature, where I is the light intensity transmitted through the sample, and I_0 is that through the ITO glass substrate. Since the transmittance contains information about the absorption as well as the scattering of light, the term $-\log(I/I_0)$ is generally termed extinction. However, the scattering effect is not important when the particle size is much smaller than the wavelength of incident light. The ordinate of Figure 2 therefore represents the absorbance. The spectra show a peak in absorbance due to the

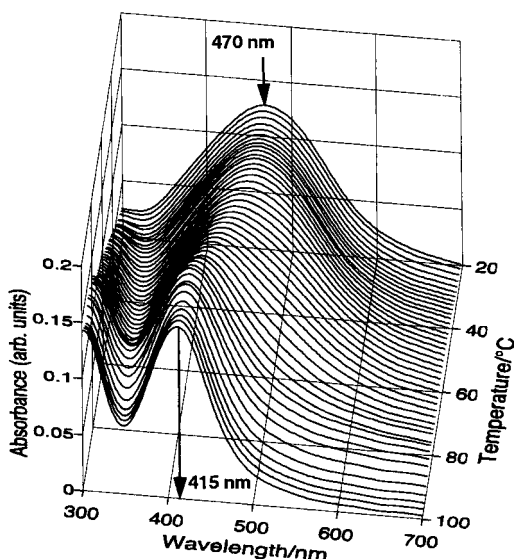


Figure 2. Changes in the optical absorption spectra calculated from the total transmittance through the sample during heat treatment. The peak wavelength of the Ag plasmon band shifted from 470 nm (at 25 °C) to 415 nm (at 100 °C) during heat treatment. Amount of Ag deposition: 11.8×10^{15} atoms cm^{-1} .

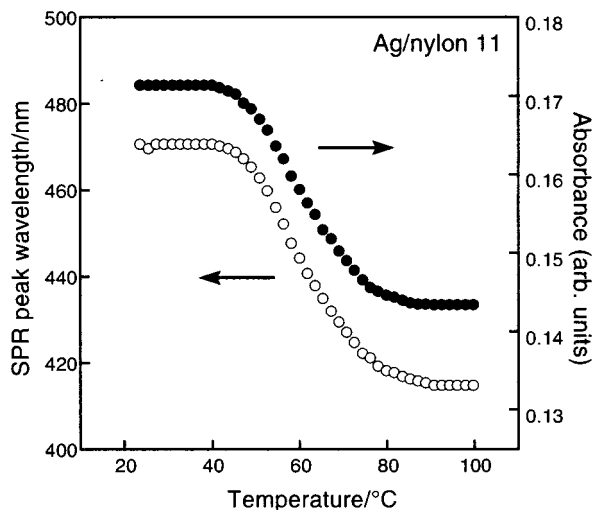


Figure 3. Variations for the peak wavelength of the Ag plasmon band and for the absorbance at the peak wavelength with temperature, obtained from the spectra shown in Figure 2.

plasmon absorption of Ag nanoparticles. The heat treatment is found to cause a shift of the plasmon peak to shorter wavelengths, decrease in absorbance, and makes the peak narrow, in good agreement with our previous results obtained for Au/nylon 11 thin film.¹⁵

The change of the peak wavelength and absorbance of the plasmon band during heat treatment is shown in Figure 3. The plasmon peak wavelength is almost constant from room temperature up to 40 °C, and shifts gradually toward shorter wavelengths from ca. 470 nm to ca. 415 nm in the temperature range 40–80 °C. In addition, the absorbance decreases simultaneously in this temperature region.

TEM Observation and Surface Stress of Ag Nanoparticles.

Figure 4 shows cross-sectional TEM images of Ag/nylon 11 thin films heat-treated at various temperatures. Before heat treatment, the Ag particles are localized at the nylon 11 surface, clearly showing the initial layered structure consisting of Ag islands deposited on the nylon 11 surface. The heat treatment at 60 °C causes the penetration of Ag particles into the nylon

11 layer, and finally we can see the homogeneous distribution of the Ag particles in the vertical direction of the nylon 11 matrix by the heat treatment at 100 °C. Particle size and size distributions of the Ag particles were obtained by counting more than 300 particles on the plan-view TEM images. Lattice constant of the particles was calculated from (220) diffraction lines on the SAED patterns, because the (220) diffraction lines are most suitable for reliable measurements of the lattice constant.¹⁸ The results are given in Table 1. The mean size of the Ag nanoparticles was 4.6 nm, and standard deviation was 1.2 nm, and appeared to be essentially unchanged upon heat treatment up to 100 °C. On the other hand, the lattice constant of the Ag particles changes slightly with heat treatment. For the as-deposited film, the lattice constant is found to be smaller than that of bulk value (4.0862 Å), indicating that the lattice contraction takes place for the Ag particles deposited on nylon 11 surface. Upon heat treatment, the lattice constant increases gradually but is still less than the bulk value. Following Vermaak et al.,¹⁹ the lattice contraction of metal particles can be interpreted in terms of surface stress. For spherical particles with a cubic structure, the surface stress f of the crystalline particle can be expressed as follows:

$$f = -\frac{3}{4} \frac{\Delta a}{a} \frac{D}{K} \quad (1)$$

where a is the lattice constant of bulk material, Δa is the change in the lattice constant due to the surface stress, K is the bulk compressibility, and D is the mean size of the particles. Using the values $a = 4.0862$ Å, $K = 9.49 \times 10^{-12}$ m²/N,²⁰ and $D = 4.6$ nm, we can calculate the surface stress coefficient of the Ag particles and the results are also given in Table 1. As the temperature increases, i.e., the Ag particles disperse from surface into the nylon 11 layer, the surface stress of the Ag particles are found to decrease from 1.43 to 0.93 N/m. These values are comparable to those obtained for silver particles deposited on carbon thin film (1.4 N/m).¹⁸

Structural Change of the Nylon 11 Matrix. Figure 5 shows the FT-IR spectrum of nylon 11 thin film deposited on Al-coated glass substrate, recorded at room temperature. The spectrum is well characterized by a bands attributed to the backbone modes together with the hydrogen-bonded amide modes of nylon 11. For the purposes of this study, we will concentrate our attention on amide I modes of the IR spectrum since the amide I mode is predominantly conformationally sensitive to local order in contrast to the conformationally insensitive N–H stretching mode, and thus suitable for the study of the structural relaxation of nylon 11 during heat treatment.^{21,22}

Temperature dependence of the FT-IR spectra in the amide I region of nylon 11 is shown in Figure 6. The spectrum at 25 °C is relatively sharp and centered at 1642 cm^{-1} . Upon an increase of temperature, the amide I mode shifts gradually to higher frequency, appears to decrease in absorbance, and becomes broader. The difference of the IR spectral features between clean and Ag-deposited nylon 11 film could not be observed, presumably due to the large fraction of nylon 11 phase relative to Ag deposited. Since there are no reports of the temperature dependence of the FT-IR spectra for vapor deposited nylon 11, the spectra can only be compared with the results of infrared temperature study of nylon 11 films casted from solution. Skrovanek et al.²² reported that the amide I mode involves three contributions related to the structural arrangement of carbonyl groups, depending on the initial state of nylon 11 and temperature, i.e., hydrogen-bonded carbonyl groups in ordered (crystalline) domains, those in disordered (amorphous)

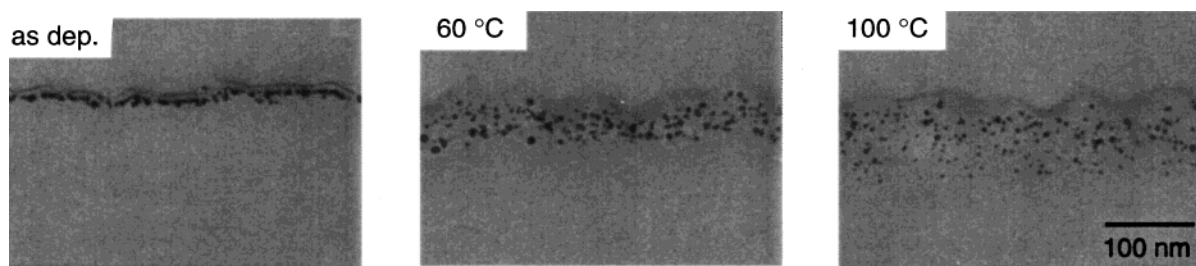


Figure 4. Cross-sectional TEM images of Ag/nylon 11 thin films heat-treated at various temperatures. Amount of Ag deposition: 11.8×10^{15} atoms cm^{-1} .

TABLE 1: Lattice Constant and Surface Stress Coefficient of the Ag Particles in the Nylon 11 Films

heat-treatment temperature ($^{\circ}\text{C}$)	lattice constant (\AA)	surface stress coefficient (N/m)
as-dep.	4.0840 ± 0.01	1.43 ± 0.2
60	4.0844 ± 0.02	1.18 ± 0.2
100	4.0848 ± 0.01	0.93 ± 0.2

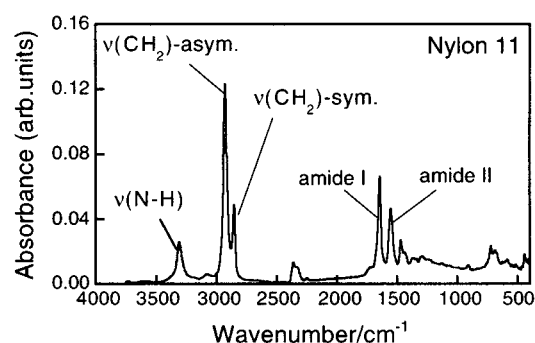


Figure 5. FT-IR spectrum of the vapor-deposited nylon 11 thin film recorded at room temperature in the range 400–4000 cm^{-1} .

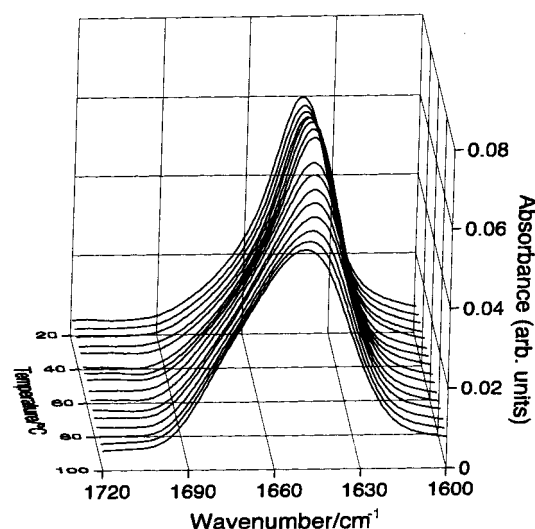


Figure 6. Changes in the FT-IR spectra of the amide I region for nylon 11 thin film, during heat treatment. The spectra were measured at temperature interval of 5 $^{\circ}\text{C}$.

conformations, and non-hydrogen-bonded (free) carbonyl groups. According to these considerations, each spectrum recorded at the different temperatures was fitted and resolved into three components by a nonlinear least-squares method adopting Gaussian peak shapes for each component. Representative examples of results for curve fitting are shown in Figure 7. At 25 $^{\circ}\text{C}$, before heat treatment, the spectral shape can be satisfactorily fitted only by two components attributable to ordered and disordered carbonyl groups, similar in form to that

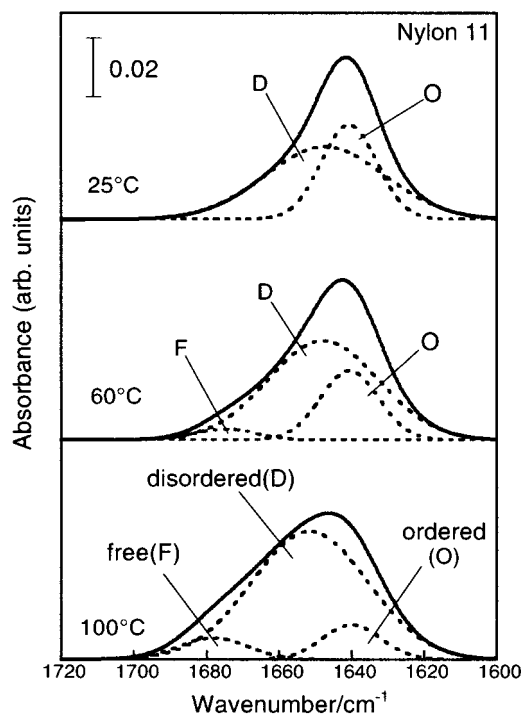


Figure 7. Curve-fitting results in the amide I region for FT-IR spectra of the vapor-deposited nylon 11 thin film. Solid line: experimental data. Dashed line: curve-fitting data.

obtained for semicrystalline nylon 11 casted from solution.²² At 60 $^{\circ}\text{C}$, in addition to the two bands at approximately 1640 and 1648 cm^{-1} , a third band attributable to the free component appears at about 1675 cm^{-1} . At 100 $^{\circ}\text{C}$, before the nylon 11 has completely melted, three bands are again necessary to fit the data.

Figure 8 shows a plot of relative areas of the three components for an amide I band as a function of temperature, obtained from the curve-fitting procedure. By heat treatment from room temperature up to 40 $^{\circ}\text{C}$, the area of the ordered and disordered bands are nearly constant, and no indication of the existence of free component is observed, i.e., only two bands are necessary to obtain a satisfactory fitting of the spectra in this temperature region. This is presumably due to that the nylon 11 films are fixed as thermodynamically metastable state since the nylon 11 molecules are quenched from the gaseous phase into the solid phase during the vapor deposition process. Significant changes of the amide I band are observed above 40 $^{\circ}\text{C}$, corresponding to the glass transition temperature, T_g , of nylon 11 (approximately 45 $^{\circ}\text{C}$). The area of the ordered band gradually decreases over a range 40–100 $^{\circ}\text{C}$. On the other hand, in the same temperature range the area of the disordered band increases in a fashion that parallels the corresponding decrease in the ordered band, and a slight and gradual increase in the

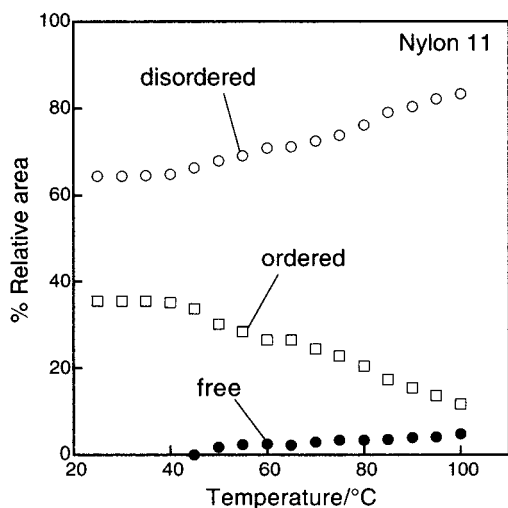


Figure 8. Temperature dependence of the areas for the ordered, disordered hydrogen-bonded, and free non-hydrogen-bonded carbonyl groups obtained from the amide I region in the FT-IR spectra shown in Figure 6.

fraction of the free component is observed. This indicates that during heat treatment up to 100 °C, a structural rearrangement of the vapor-deposited nylon 11 film occurs, leading to a decrease in the degree of crystallinity of the nylon 11 and a corresponding increase in the fraction of amorphous phase. Although not shown here, the ordered component vanished and there was an obvious increase in the amount of amorphous component (disordered and free) above 120 °C, indicating complete melting of the nylon 11 matrix. However, the melting point of semicrystalline nylon 11 prepared from solution is ca. 190 °C.²² This difference of the melting behavior may be caused by the difference of molecular weight of the nylon 11 polymer, i.e., nylon 11 was degraded during vapor deposition process and thus obtained with lower molecular weight compared with the nylon 11 prepared from solution. These results clearly demonstrated that the vapor-deposited nylon 11 thin film are metastably fixed and semicrystalline, including hydrogen-bonded small crystallites, and relaxed upon heat treatment above 40 °C. Our previous room-temperature TEM observation and high-resolution electron diffraction analysis revealed that, after heat treatment at various temperature, needlelike α -crystalline phase appeared in the nylon 11 films.¹⁶ However, since the degree of crystallinity of the nylon 11 decreases during heat treatment, the crystallization to the α -form is believed to occur during the cooling process.

Discussion. The results of optical transmission measurement and TEM observation demonstrate that the shift of the plasmon absorption is closely related to the dispersion state of the Ag particles in the film. As is generally known, the plasmon absorption features of metal nanoparticles dispersed in dielectric medium are associated with the effective dielectric constant of the composite, which are the function of several parameters, e.g., size and shape of the nanoparticles, volume fraction of metal phase, and dielectric constant of surrounding medium.^{4–8} The dielectric constant of metals depends on particle size due to the scattering of free electrons at the particle surface.²³ However, since the mean size of the Ag particles presently studied is mostly unchanged upon heat treatment, such effect would not be significant. In addition, the dielectric constant of the nylon 11 matrix appeared to be only slightly changed upon heat treatment, as proven by the ellipsometric measurements.¹⁵ Therefore, the shift of the plasmon peak is considered to be mainly caused by the changes in the distribution of the Ag

particles in the film. The penetration of the Ag particles with constant particle number leads to a relative decrease of particle concentration per unit volume, since interparticle distance increases as the Ag particles disperse into the matrix. As a result, the local volume fraction of the Ag particles in the films decreases gradually as the particles disperse into the nylon 11 layer. This change in the volume fraction of Ag particles results in the change in the effective dielectric constant of the composite film because the interaction of dipoles induced in the particles by external electromagnetic field of incident light depends on the distance between neighboring particles. The observed changes in the absorption spectra shown in Figure 2 can be, therefore, qualitatively explained by the changes in the effective dielectric constant of the Ag/nylon 11 composite film, which is caused by the decrease of average local volume fraction of the Ag particles during heat treatment. This effect can also be responsible for the decrease of the plasmon band intensity and width during heat treatment.

From the above considerations, it seems likely that the plasmon peak position begins to shift to shorter wavelengths at the temperature at which the Ag particles penetrate into the matrix. Namely, from the results shown in Figure 3, the Ag particles fixed initially at the nylon 11 surface begin to penetrate and embed into the nylon 11 matrix at 40 °C, and homogeneously distribute in the whole of the film at 80 °C.

For the Ag particles to disperse into the nylon 11 matrix, there must be a driving force for embedding of the particles from the nylon 11 surface, i.e., the surface Gibbs free energy of the Ag particle inside the polymer phase must be lower than that of the particle at the surface. In order for the penetration of the Ag particles into the nylon 11 phase to be energetically favorable, the following relation must be satisfied:^{24,25}

$$\gamma_{\text{Ag}} > \gamma_{\text{Ag-nylon}} + \gamma_{\text{nylon}} \quad (2)$$

i.e., the surface tension of the Ag particle, γ_{Ag} , must exceed the sum of the interfacial tension, $\gamma_{\text{Ag-nylon}}$, and the surface tension of the nylon 11, γ_{nylon} . If the inequality (eq 2) holds, nylon 11 matrix can wet completely the surface of the Ag particle. If the surface stress can be interpreted as an isotropic surface stress, the relation between surface tension and surface stress is expressed as follows:^{26,27}

$$f = \gamma + \frac{d\gamma}{de} \quad (3)$$

where $d\gamma/de$ represents the dependence of γ on the elastic strain e . The surface tension of silver at room temperature can be found by using Eötvös's rule²⁸ to extrapolate the value of 1.2 J/m² near the melting temperature.²⁹ This yields a value of 1.6 J/m² at 25 °C, which is slightly higher than the surface stress of the Ag particles found in the present study (Table 1). The $d\gamma/de$ is thus negative, derived from eq 3. The results indicate that the stress in the Ag particle surface due to the exposure of the surface atoms is one of the compression. This tendency is generally evident, i.e., that in crystals, $d\gamma/de$ is intrinsically negative as was also found experimentally for Au nanoparticles dispersed in nylon 11 films.¹⁶ In the present study, moreover, the surface stress coefficient of the Ag particles was found to decrease as the particles disperse into the matrix, due to the increase of the lattice constant with the fixed particle size. Drechsler and Nicholas³⁰ reported by a theoretical investigation that the increase of the lattice constant due to hydrostatic pressure results in a decrease of the surface tension. Therefore, we suggest that the dispersion of the Ag particles can be

attributed to the reduction of the high surface free energy of the particles by embedding, i.e., there is a driving force originating from inequality (eq 2) for the Ag particles to embed below the nylon 11 surface. We note here that the penetration of Ag particles seems to occur under specific condition, although the inequality (eq 2) is obeyed by many metal/polymer systems because surface tension of polymers is generally very small in comparison to surface tension of metals. The results of IR studies demonstrate that the vapor-deposited nylon 11 films are semicrystalline and fixed in a glassy state, indicating that hydrogen-bonded molecular chains are immobile up to 40 °C (T_g) so that the nylon 11 matrix cannot wet the Ag particles at this temperature region. Therefore, the inequality (eq 2) can only be obeyed when the temperature rises above the T_g at which the nylon 11 matrix begin to behave as a viscous fluid. With increasing temperature above the T_g , the free component appeared to be increased. This clearly indicates the nylon 11 matrix to be much softened, providing sufficient mobility toward the Ag particles for further dispersion through viscous flow of the matrix. Further experimental study is, however, necessary in order to quantitatively evaluate the motion of the particles in polymer matrix. In particular, more detailed information associated with the particle mobility and penetration rate can be obtained from an experiment with respect to the dependence of heating rate and time on the optical and vibrational characteristics of metal/polymer interface, which are currently under way and results will be published elsewhere.

Summary

We have studied the effect of heat treatment on dispersion of Ag nanoparticles into nylon 11 thin film by means of in situ optical and vibrational spectroscopy as well as microscopic analysis. The shift of the plasmon peak originated from the Ag particles to shorter wavelength were clearly observed during heat treatment, which can be explained by the changes in the effective dielectric constant of the composite film, due to the reduction of the effect of dipole interaction between neighboring particles. It was also found that the vapor-deposited nylon 11 thin films are in a thermodynamically metastable state and relaxed to a much more stable state upon heat treatment. The Ag particles were observed to penetrate from surface into bulk phase of the nylon 11 matrix when the samples are heat-treated at temperatures which are above the glass transition temperature of nylon 11 because nylon 11 can wet completely the Ag particles. The decrease of the surface stress coefficient of the Ag particles by embedding into nylon 11 layer, as determined from lattice constant of the Ag particles, is consistent with this results.

The present study revealed that there is a correlation between the temperature at which the plasmon peak begin to shift and the nylon 11 matrix relaxes. From an experimental point of view, these results demonstrate the applicability of the in situ spectroscopic technique to the study of dispersion phenomena of metal nanoparticles by the thermal relaxation technique; for instance, one can estimate the temperature at which metal nanoparticles begin to penetrate into polymer matrix.

References and Notes

- (1) Dremus, R. H. *J. Chem. Phys.* **1964**, *40*, 2389.
- (2) Granquist, C. G.; Hunderi, O. *Phys. Rev. B* **1977**, *16*, 3513.
- (3) Brus, L. E. *J. Chem. Phys.* **1984**, *80*, 4403.
- (4) Kreibig, U.; Ganzel, L. *Surf. Sci.* **1985**, *156*, 678.
- (5) Hayashi, S.; Koga, R.; Ohtuji, M.; Yamamoto, K.; Fujii, M. *Solid State Commun.* **1990**, *76*, 1067.
- (6) Wang, Y.; Herron, N. *J. Phys. Chem.* **1991**, *95*, 525.
- (7) Takeuchi, Y.; Ida, T.; Kimura, K. *J. Phys. Chem.* **1997**, *101*, 1322.
- (8) Palpant, P.; Prével, B.; Lermé, J.; Cottancin, E.; Pellarin, M.; Treilleux, M.; Perez, A.; Vialle, J. L.; Broyer, M. *Phys. Rev. B* **1998**, *57*, 1963.
- (9) Raether, H. *Surface Plasmons on Smooth and Rough Surfaces and on Gratings*; Springer-Verlag: Berlin, 1988.
- (10) Kume, T.; Amano, T.; Hayashi, S.; Yamamoto, K. *Thin Solid Films* **1995**, *264*, 115.
- (11) Kume, T.; Hayashi, S.; Yamamoto, K. *Mater. Sci. Eng.* **1996**, *A217*, 171.
- (12) Noguchi, T.; Gotoh, K.; Yamaguchi, Y.; Deki, S. *J. Mater. Sci. Lett.* **1991**, *10*, 477.
- (13) Noguchi, T.; Gotoh, K.; Yamaguchi, Y.; Deki, S. *J. Mater. Sci. Lett.* **1991**, *10*, 648.
- (14) Akamatsu, K.; Deki, S. *J. Mater. Chem.* **1997**, *7*, 1773.
- (15) Akamatsu, K.; Deki, S. *J. Mater. Chem.* **1998**, *8*, 637.
- (16) Akamatsu, K.; Deki, S. *J. Colloid Interface Sci.* **1999**, *214*, 353.
- (17) Kreibig, U.; Vollmer, M. *Optical Properties of Metal Clusters*; Springer-Verlag: Berlin, 1995; p 13.
- (18) Mays, C. W.; Vermaak, J. S.; Kuhlmann-Wilsdorf, D. *Surf. Sci.* **1968**, *12*, 134.
- (19) Vermaak, J. S.; Mays, C. W.; Kuhlmann-Wilsdorf, D. *Surf. Sci.* **1968**, *12*, 128.
- (20) *Gmelins Handbook of Inorganic Chemistry*; VCH: Weinheim, 1970; p 225.
- (21) Skrovanek, D. J.; Howe, S. E.; Painter, P. C.; Coleman, M. M. *Macromolecules* **1985**, *18*, 1676.
- (22) Skrovanek, D. J.; Howe, S. E.; Painter, P. C.; Coleman, M. M. *Macromolecules* **1986**, *19*, 699.
- (23) Kreibig, U.; Fragstein, C. V. *Z. Physik* **1969**, *224*, 307.
- (24) Kovacs, G. J.; Vincett, P. S.; Tremblay, C.; Pundsack, A. L. *Thin Solid Films* **1983**, *101*, 21.
- (25) Faupel, F. *Phys. Status Solidi A* **1992**, *134*, 9.
- (26) Shuttleworth, R. *Proc. Phys. Soc. London* **1950**, *A63*, 444.
- (27) Herring, C. *The Structure and Properties of Solid Surfaces*; Gomer, R., Smith, C. S., Eds.; University of Chicago Press: Chicago, 1952; p 5.
- (28) Adam, N. K. *Physics and Chemistry of Surfaces*; Dover: New York, 1968; p 158.
- (29) Funk, E. R.; Udin, H.; Wulff, J. *J. Metals* **1951**, *3*, 1206.
- (30) Drechsler, M.; Nicholas, J. F. *J. Chem. Phys. Solids* **1967**, *28*, 2609.